
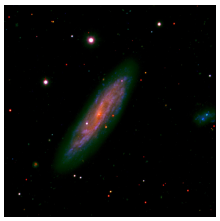
LBT & Image

"X-RAY SPECTROSCOPY OF GOLD NANOPARTICLES"

Sultana N. Nahar

Astronomy: Anil Pradhan, M. Montenegro
Chemistry: R.M. Pitzer
The Ohio State University
Columbus, Ohio, USA

"64th International Symposium on Molecular Spectroscopy"
Ohio State University, Columbus, Ohio, USA
June 22-26, 2009

Support: Large Interdisciplinary Grant - OSU, NASA APRA
Computations - Ohio Supercomputer Center (OSC), Columbus, Ohio

GOLD NANOPARTICLES

- Nanoparticles- common in biomedical applications
- Radiation therapy with nanoparticles embedded in a cancer tumor is more effective than pure irradiation since the nanoparticles can absorb X-rays and produce secondary electrons and photons that kill the surrounding malignant cells
- Inner shell transitions, such as 1s-2p, in heavy elements absorb or produce high energy X-rays $\rightarrow$ heavy elements are widely used in nanoparticles
- Gold nanoparticles are common in biomedical applications - because of (i) non-reactive to body tissue, (ii) absorb hard X-rays that can have deeper tissue penetration, (iii) hard X-rays are transparent to body elements, such as, H, O, C, N, K, Fe
- Investigations have been carried out to find the enhancements in X-ray absorption by the nanoparticles, mainly at the K-shell ionization energy
- Our study focuses - Resonant Absorption due to 1s-np photo-excitations below the K-shell energy
- Aim: Larger production of Electrons and Photons - Ejection of an 1s electron can lead to Auger cascade of emission of photons and electrons

PHOTOIONIZATION: X(ion) + $h\nu \rightarrow X^+ + e$

K-SHELL EDGE EFFECT ON X-RAY ABSORPTION BY GOLD NANOPARTICLES & WATER

- **Figure shows** *background photoinization* **(resonance excluded) cross sections σ_{PI} of gold & water**
- **Rises in σ_{PI} correspond to enhancements in ionization at various K, L, M (sub)-shells energies**
- **Oxygen K-edge is at 0.53 keV - rise is not seen**
- **Au K-shell ionization edge $\sim$ 81 keV (studied for enhanced ionization & follow-up emissions)**
- **σ_{PI} peak at K-shell threshold is small in magnitude - the reason for no observation of appreciable rise in X-ray photon absorption**

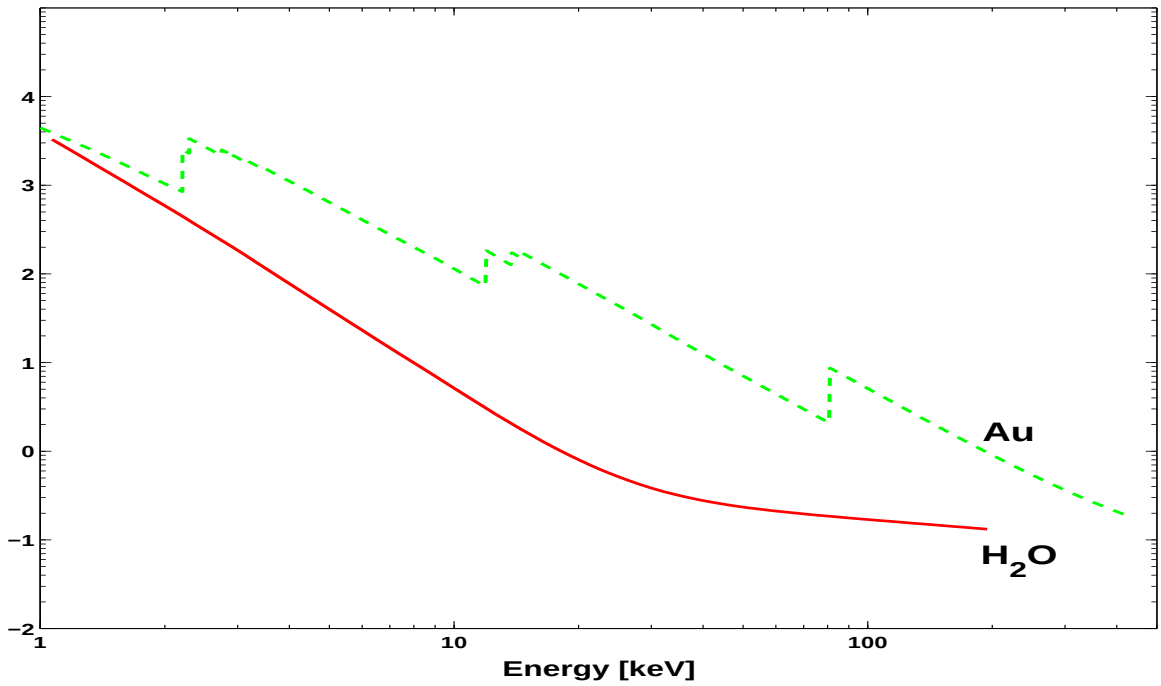

Auger Cascade: ELECTRON & PHOTON EMISSIONS

Auger Process: An electron from a higher level drops to fill a lower level vacancy, but emits a photon that can knock out another electron. This can lead to cascade as the vacancies move upward, more electrons and photons are emitted.

- **Fig (i) Ionization by X-ray photons (E_X) ($>$ K-shell ionization energy E_K) leading to Auger process**
- **Fig (ii) Multiple electron vacancies due to successive Auger decays leading to emission of photons and electrons**
- **Single ionization of 1s electron can lead to ejection of 20 or more electrons in an ion with occupied O and P shells**
- **Fig (iii) Inverse to Auger - Resonant photo-excitation from 1s $\rightarrow$ 2p (with L-shell vacancy) by an external monoenergetic X-ray source with intensity above our predicted critical flux**

$$\Phi^{c}(\nu_{K\alpha}) = \frac{\sum_{n_i \geq 2} g_i A[n_i(S_i L_i J_i) \rightarrow 2(SLJ)]}{g_K B_{K\alpha}}. \qquad (1)$$

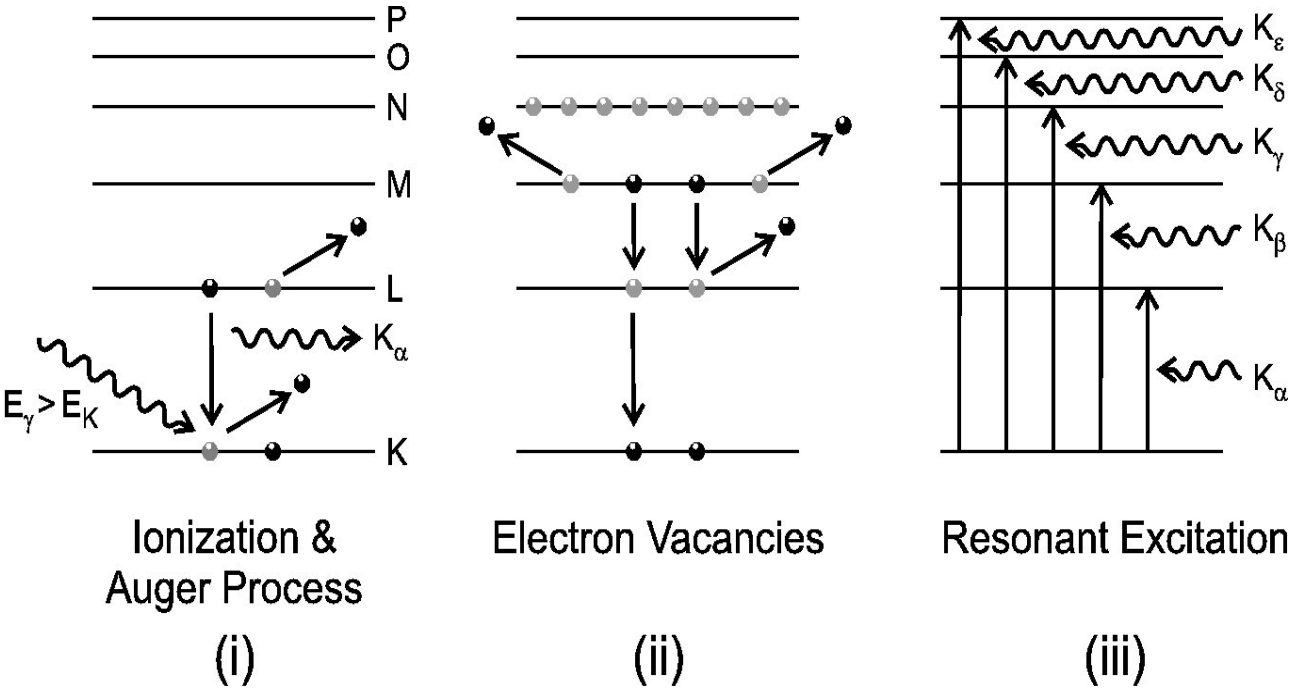

X-RAY INTERACTION WITH GOLD NANOPARTICLES

1. Photoexcitation:

$$X^{+Z} + h\nu \rightleftharpoons X^{+Z*}$$

- **Oscillator Strength (f), Radiative Decay Rate (A-value)**

2. Direct Photoionization (PI) :

$$X^{+Z} + h\nu \rightleftharpoons X^{+Z+1} + \ e$$

3. Photoionization via an Autoionizing State :

$$e + X^{+Z} \rightleftharpoons (X^{+Z-1})^{**} \rightleftharpoons \begin{cases} e + X^{+Z} & \text{AI} \\ X^{+Z-1} + h\nu & \text{DR} \end{cases}$$

The doubly excited state - "autoionizing state" - introduces resonances

- 2 & 3. **Photoionization Cross Sections (σ_{PI})**

FOR MONTE CARLO SIMULATIONS:

- 4. **Compton Scattering (significant for body elements):**

$$h\nu + X^{+Z} \rightleftharpoons (X^{+Z})^* + h\nu'$$

5. Secondary Electron Collisions:

Ionization: $e + X^{+Z} \rightarrow e' + e" + X^{+Z+1}$
Excitation: $e + X^{+Z} \rightarrow e' + X^{+Z*}$

THEORY

For a multi-electron system, in nonrelativistic LS coupling:

$$H^{NR}\Psi = \left[\sum_{i=1}^{N}\left\{-\nabla_i^2 - \frac{2Z}{r_i} + \sum_{j>i}^{N}\frac{2}{r_{ij}}\right\}\right]\Psi = E\Psi. \tag{2}$$

Relativistic effects: For a multi-electron system, the Breit-Pauli Hamiltonian is:

$$H_{\rm BP} = H_{NR} + H_{\rm mass} + H_{\rm Dar} + H_{\rm so}+$$

$$\frac{1}{2}\sum_{i\neq j}^{N}[g_{ij}(so+so') + g_{ij}(ss') + g_{ij}(css') + g_{ij}(d) + g_{ij}(oo')]. \tag{3}$$

where the Breit interaction is

$$H^B = \sum_{i>j}[g_{ij}(so+so') + g_{ij}(ss')] \tag{4}$$

and one-body corrections terms are

$H^{mass} = -\frac{\alpha^2}{4}\sum_i p_i^4$, $H^{Dar} = \frac{\alpha^2}{4}\sum_i \nabla^2\left(\frac{Z}{r_i}\right)$, $H^{so} = \left[\frac{Ze^2\hbar^2}{2m^2c^2r^3}\right]$ **L.S**

Wave functions and energies are obtained solving:

$$\mathbf{H\Psi = E\Psi}$$

- **E** $< 0 \rightarrow$ **Bound (e+ion) states** Ψ_B
- **E** $\geq 0 \rightarrow$ **Continuum states** Ψ_F

Transition Matrix elements with dipole operator $\mathbf{D} = \sum_i \mathbf{r}_i$,

$< \Psi_B||\mathbf{D}||\Psi_{B'} >$ $\rightarrow$ **Radiative Excitation and Deexcitation**

$< \Psi_B||\mathbf{D}||\Psi_F >$ $\rightarrow$ **Photoionization and Recombination**

The matrix element reduces to generalized line strength,

$$\mathbf{S} = \left| \left\langle \Psi_\mathbf{f} | \sum_{\mathbf{j}=1}^{\mathbf{N}+1} \mathbf{r_j} | \Psi_\mathbf{i} \right\rangle \right|^2 \tag{5}$$

Oscillator Strength. Cross Section, Attenuation Coefficient

• The oscillator strength (f_{ij}) and radiative decay rate (A_{ji}) for the bound-bound transition are

$$\mathbf{f_{ij}} = \left[\frac{\mathbf{E_{ji}}}{\mathbf{3g_i}}\right] \mathbf{S}, \quad \mathbf{A_{ji}(sec^{-1})} = \left[\mathbf{0.8032 \times 10^{10}} \frac{\mathbf{E_{ji}^3}}{\mathbf{3g_j}}\right] \mathbf{S} \tag{6}$$

• The resonant structures of $K\alpha, K\beta, K\gamma, K\delta, K\eta$ complexes in photoionization cross sections σ_{PI} are obtained from Auger line strengths. For this, the resonant cross sections were convolved over a normalized gaussian function

$$\sigma_{\mathbf{K}\alpha}(\nu; \mathbf{K} \rightarrow \mathbf{L_i}) = \frac{\mathbf{4\pi^2 a_o^2 \alpha}}{\mathbf{3}} \frac{\mathbf{E(K - L_i)}}{\mathbf{g_k}} \mathbf{S(K - L_i)} \phi(\nu) \tag{7}$$

where $\phi(\nu)$ the Gaussian profile,

$$\phi(\nu) = \frac{\mathbf{1}}{\sqrt{\mathbf{2\pi}}\mathbf{\Delta E}} \exp\left(-\frac{\mathbf{E^2}}{\mathbf{2\ \Delta E^2}}\right)$$

• The mass attenuation coefficient per volume mass, κ is

$$\kappa_{\mathrm{res}}(\nu; \mathbf{K}\alpha) = \frac{\sum_\mathbf{j} \mathbf{w_j} \sum_\mathbf{i} \sigma_{\mathrm{res}}(\nu; \mathbf{K - L_{ji}})}{\mathbf{u W_A} \sum_\mathbf{j} \mathbf{w_j}} \tag{8}$$

where u is 1 amu, W_A = atomic weight, w_j=statistical weight

RESONANT K_α $(1s-2p)$ TRANSITIONS IN Au (Nahar et al 2008)

- **The table presents data for resonant K_α $(1s-2p)$ transitions in Au and Fe from Hydrogen-like to Flourine-like ionization states.**
- **Number of $1s-2p$ transitions or resonances, N_T, varies with ionic states**
- **The resonant energy, $E(K_\alpha)$, and the corresponding photoionization cross section, $\sigma_{res}(K_\alpha)$ are obtained from statitical averaging**
- **These resonance strengths provide the dominant contribution to photo-absorption, far above the background**

			Fe		Au	
Ion Core	Transition Array	# of Transitions	$E(K_\alpha)$ (keV)	$\langle\sigma_{res}(K_\alpha)\rangle$ (Mb)	$E(K_\alpha)$ (keV)	$\langle\sigma_{res}(K_\alpha)\rangle$ (Mb)
F-like	$1s^22s^22p^5 - 1s2s^22p^6$	2	6.6444	1.33	68.324	0.99
O-like	$1s^22s^22p^4 - 1s2s^22p^5$	14	6.5096	5.80	68.713	4.10
N-like	$1s^22s^22p^3 - 1s2s^22p^4$	35	6.5237	10.12	68.943	5.17
C-like	$1s^22s^22p^2 - 1s2s^22p^3$	35	6.5633	12.86	69.136	8.63
B-like	$1s^22s^22p^1 - 1s2s^22p^2$	14	6.5971	7.11	68.938	3.48
Be-like	$1s^22s^2 - 1s2s^22p$	2	6.6375	5.36	68.889	3.47
Li-like	$1s^22s - 1s2s2p$	6	6.6617	5.02	68.893	2.82
He-like	$1s^2 - 1s2p$	2	6.6930	6.01	68.703	3.93
H-like	$1s - 2p$	2	6.9655	2.18	69.663	1.58

X-ray Absorption Spectra of Gold Nanoparticles
(Pradhan et al. 2009)

• **Figure shows X-ray mass absorption coefficient $\kappa(cm^2/g)$ of resonant K-shell complexes, K $\rightarrow$ L, M, N, O, P transitions (E = 67.5 - 79 keV), and non-resonant background for He-like to F-like gold ions (with 2s, 2p-subshell vacancies) below the K-edge ($\geq$ 80.729 keV) of the ions**

• **Photo-absroption by the resonant K-complexes exceeds the background below the K-edge ionization by up to $\sim 10^3$**

• **Note, not studied before, that the K-ionization jump is orders of magnitude smaller than resonant cross sections**

• **Thus, compared to resonant energies continuum X-ray opacity in the high-energy regime is generally small.**

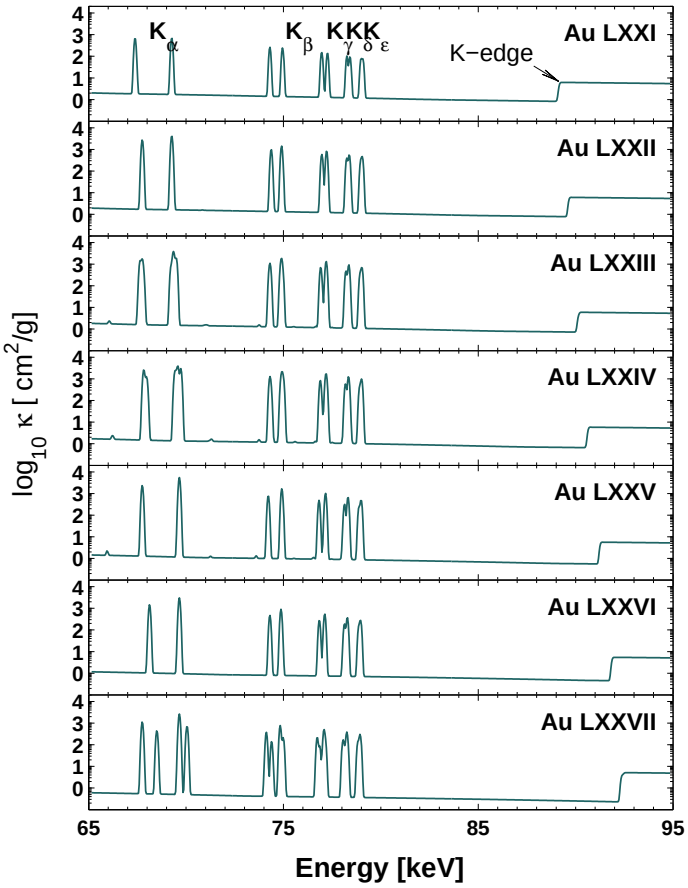

Monte Carlo Simulation for Resonant K_α X-Ray Absorption by Au Nanoparticles

(Montenegro et al. 2009)

- We applied gold κ in Monte Carlo simulation to study X-ray absorptions and intensities of emitted photons and electrons by Auger process in tissues
- We modifed the simulation code, GEANT4, to include the resonant cross sections
- TOP: Geomtry of the experiment - the phantom (15 x 5 x 5 cm) models a tumor embedded with gold nanoparticles (golden section 2 cm) 10 cm inside normal tissue (blue section)
- BOTTOM: Simulation - gold nanoparticles at 5 mg/ml, X-ray beam at resonant energy $\sim$ 68 keV
- NOTE: Because of Compton scattering only a few photons reach the region with gold nanoparticles

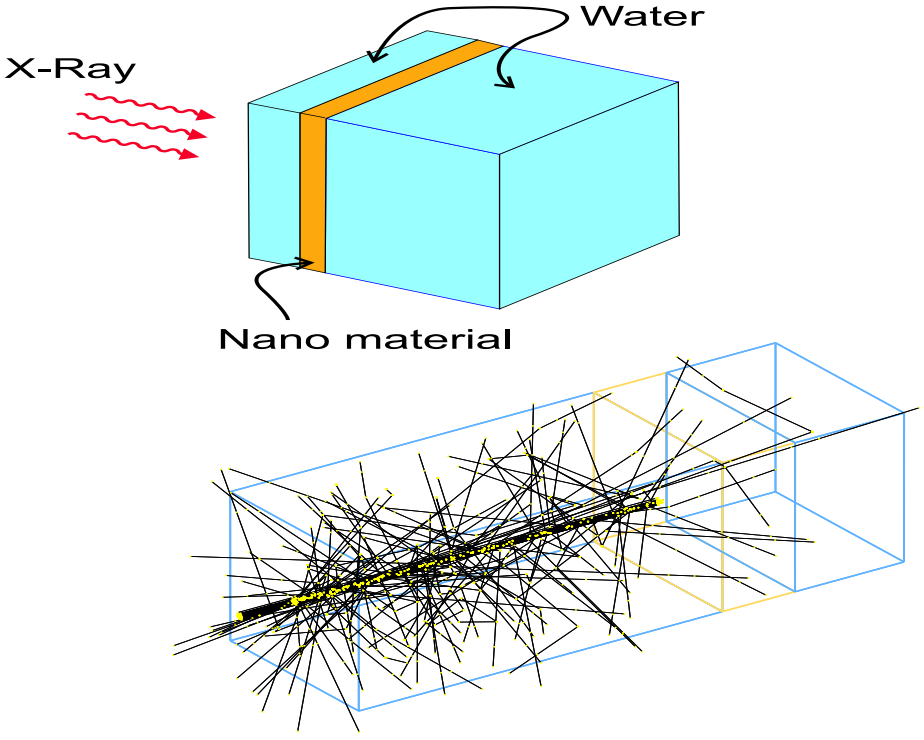

X-RAY ABSORPTION BY Au AT 68 keV, 82 keV, 2 MeV

Figure: X-ray energy deposited by depth in the phantom: Red curve - with tumor in region 100 to 120 mm embedded with gold nanoparticles at 5 mg/ml, Blue curve - only water

- **Top:** X-ray at 68 keV - averaged Kα resonant energy
- **Middle:** 82 keV - just above K-edge ionization energy
- **Bottom:** 2 MeV - high energy common in clinical usage
- The presence of gold nanoparticles has increased the energy deposited at the tumor
- The highest absorption, by more than 25 time that at 82 keV, is at the resonant energy 68 keV (top panel)

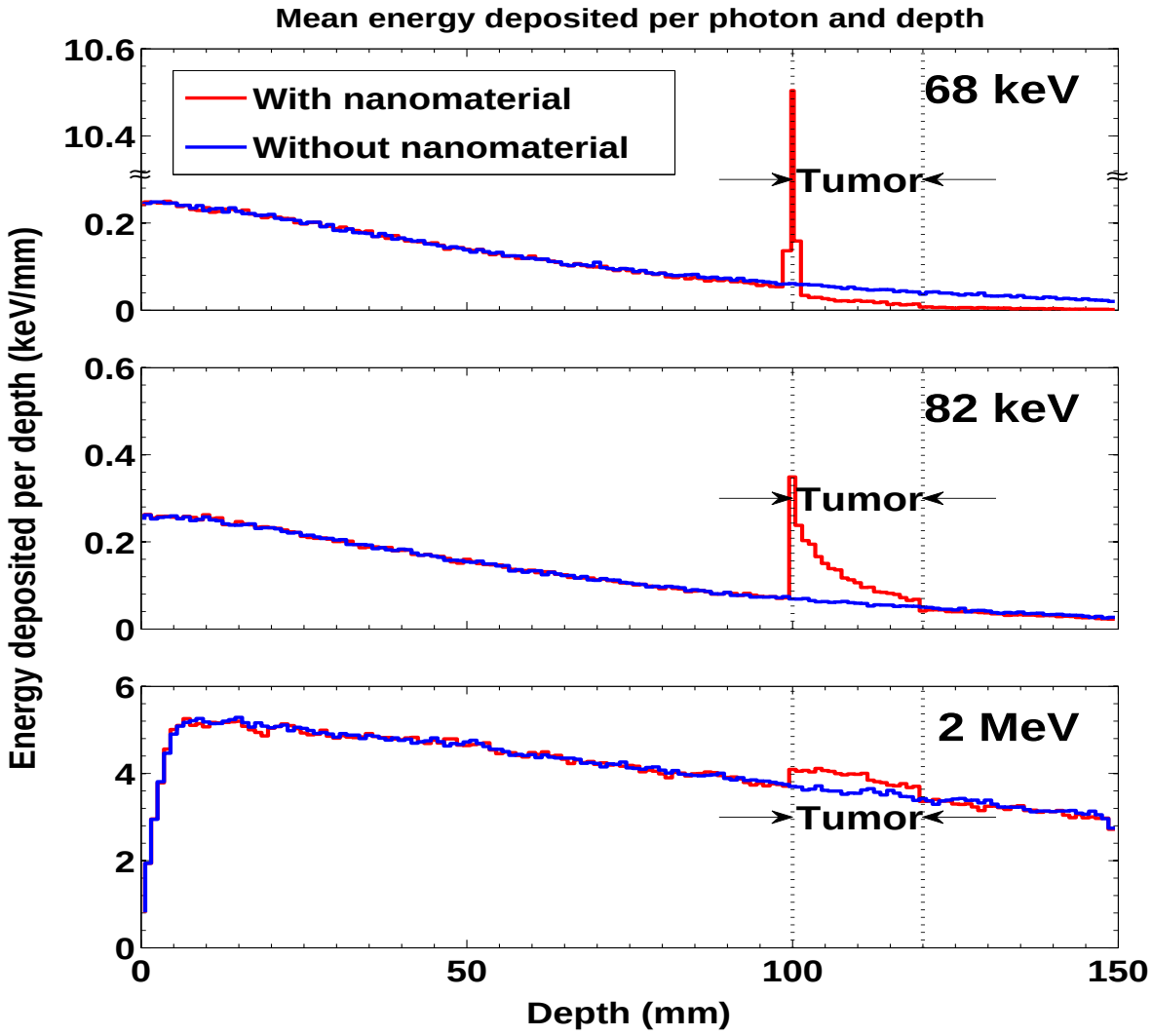

ELECTRON PRODUCTIONS AT 68 keV, 82 keV, 2 MeV

Figure: Number of Auger electrons produced with depth following X-ray absorptions: Red curve - tumor embedded with gold nanoparticles at 5 mg/ml in region 100 to 120 mm, Blue curve - only water

- **Top:** X-ray at 68 keV - averaged Kα resonant energy
- **Middle:** 82 keV - just above K-edge ionization energy
- **Bottom:** 2 MeV - high energy common in clinical usage
- A considerably large number of electrons, by more than an order of mangitude, were produced by 68 keV X-rays compared to those by 82 keV and 2 MeV

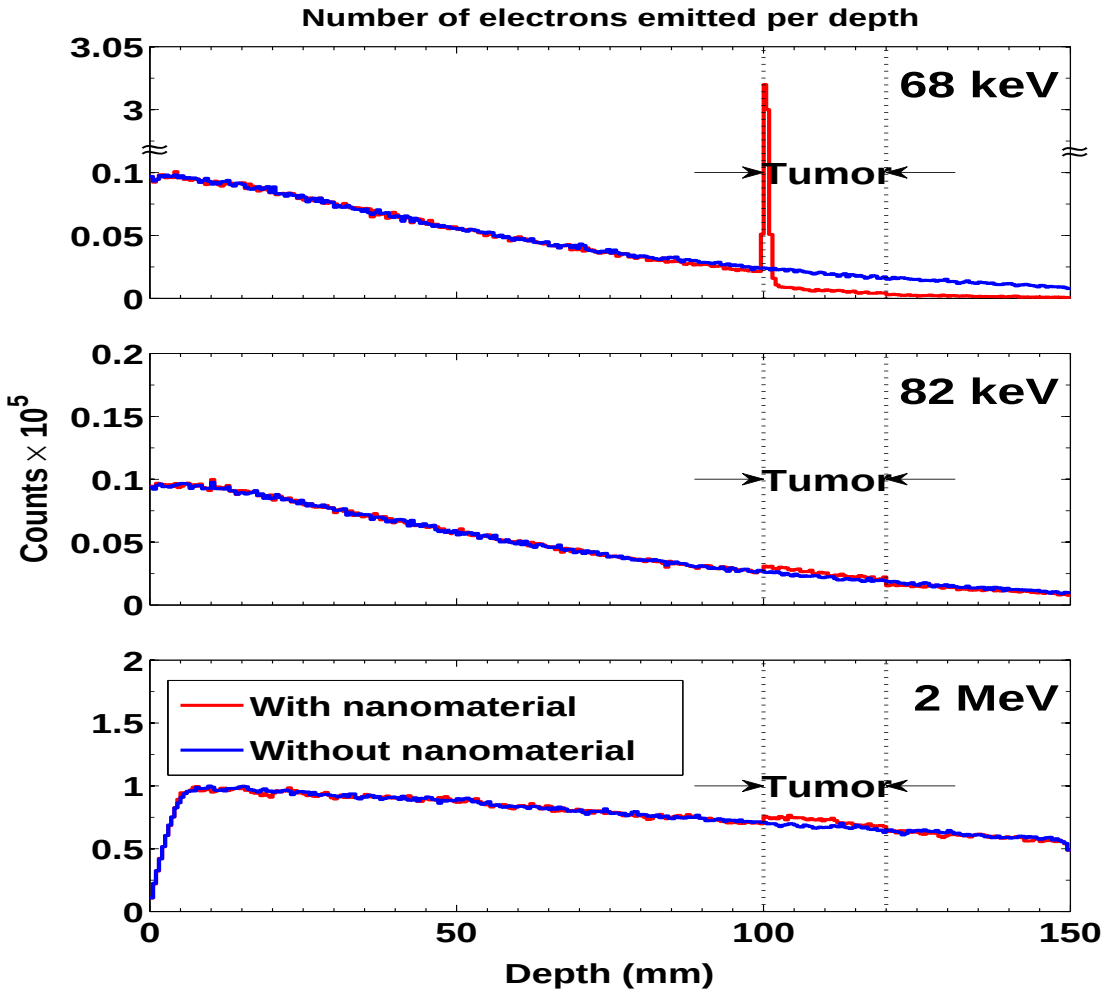

PHOTON PRODUCTIONS AT 68 keV, 82 keV, 2 MeV

Figure: Number of Auger photons produced with depth following X-ray absorptions: Red curve - tumor embedded with gold nanoparticles at 5 mg/ml in region 100 to 120 mm, Blue curve - only water

- **Top:** X-ray at 68 keV - averaged Kα resonant energy
- **Middle:** 82 keV - just above K-edge ionization energy
- **Bottom:** 2 MeV - high energy common in clinical usage
- While 82 keV and 2 MeV X-rays are showing almost no enhancement in photon production by the nanoparticles in the tumor region, a surge of photon production can be seen for the 68 keV curve.

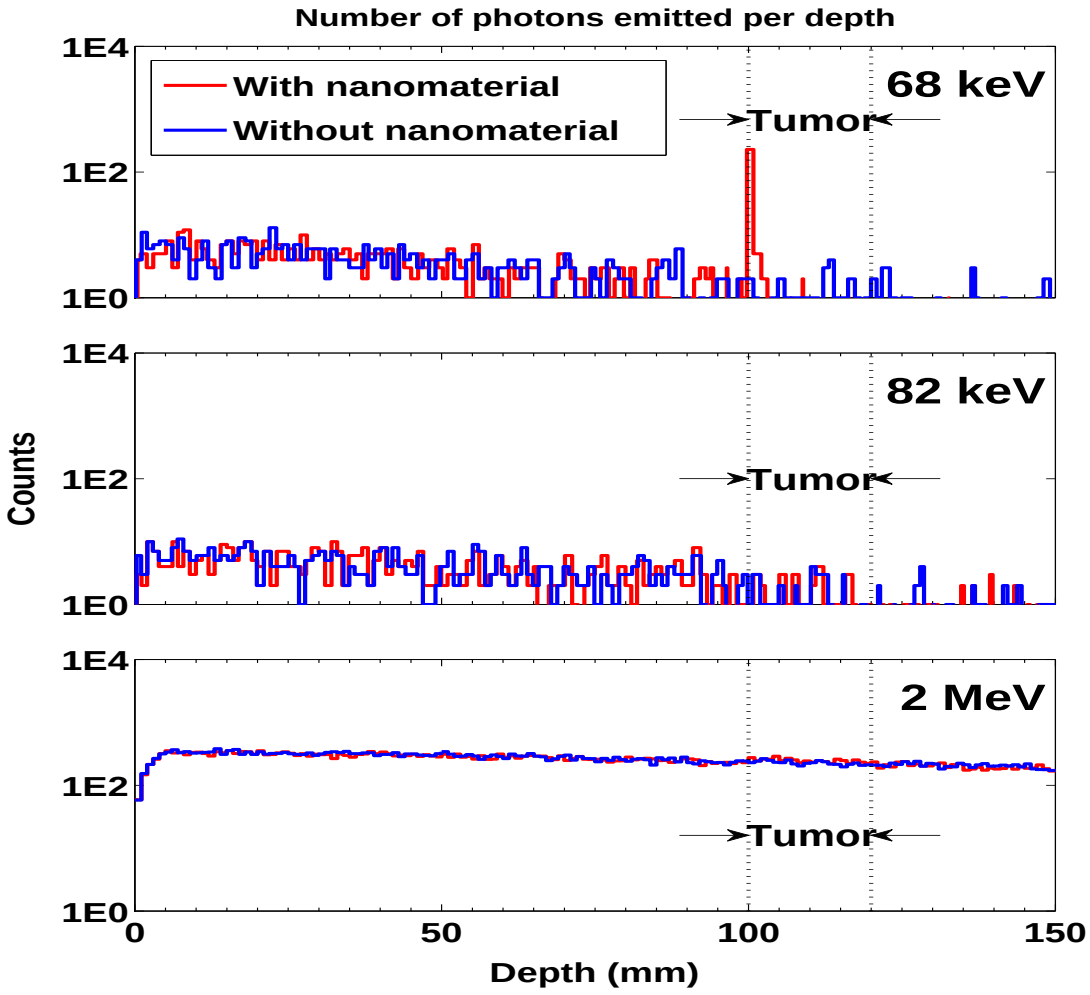

Radiation Dose Enhancement Factor (DEF)

DEF is the ratio of the average radiation dose absorbed by the tumor when it is loaded with a contrast medium or agent (viz. iodine) to the dose absorbed without that agent

Figure: DEFs with various gold nanoparticle concentration from 0 to 50 mg/ml

- Red: X-ray at 68 keV - averaged Kα resonant energy
- Green: 82 keV - just above K-edge ionization energy
- Blue: 2 MeV - high energy common in clinical usage
- The DEFs obtained for the resonant X-ray beam of 68 keV are one order of magnitude greater than those calculated at lower concentration using iodine as a contrast agent.

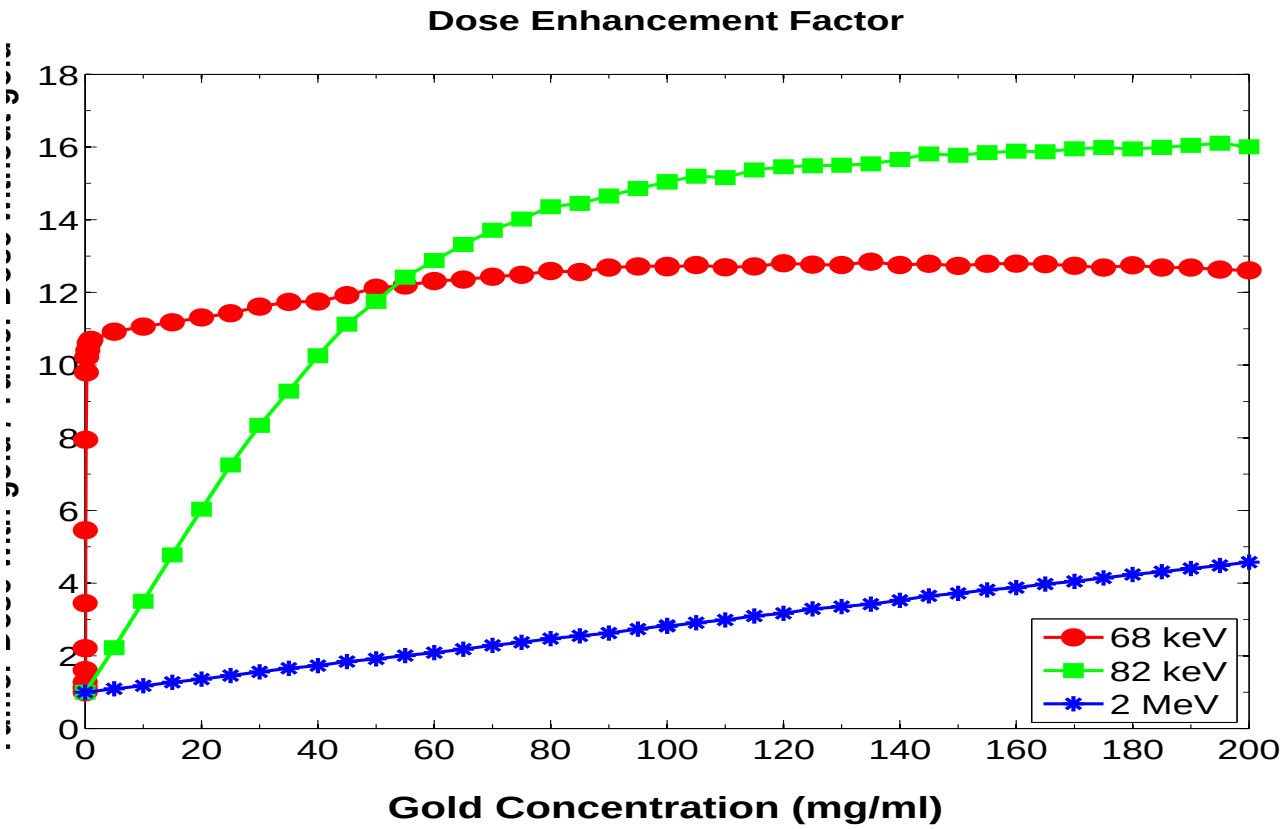

CONCLUSION

1. • **We present X-ray spectroscopy of gold nanoparticles for biomedical applications. We predict resonant energies below the K-shell ionization threshold and ehanced X-ray absorption at these energies**
2. **We have calculated Auger resonant probabilities and cross sections to obtain total mass attenuation coefficients with resonant cross sections and detailed resonance structures corresponding to $K\alpha, K\beta, K\gamma, K\delta, K\eta$ complexes lying between 67-80 keV in gold**
3. **We found that the attenuation coefficients for X-ray absorptions at resonant energies are much larger, by orders of magnitude, higher over the background cross section as well as to that at K-edge threshold**
4. **We have modied the Monte Carlo simulation code GEANT4 to accomodate the resonances**
5. **The simulation shows predicted results of enhanced X-ray absorption and follow-up enhanced electron and photon emissions. The average enhancement at the resonant energy 68 keV is up to a factor of thousand or more for associated $\mathrm{K} \rightarrow \mathrm{L}, \mathrm{M}, \mathrm{N}, \mathrm{O}, \mathrm{P}$ transitions**